

CORTICAL SURFACE DIFFUSION GENERATIVE MODELS

Zhenshan Xie, Simon Dahan, Logan Z. J. Williams, M. Jorge Cardoso, Emma C. Robinson

King’s College London
School of Biomedical Engineering & Imaging Science

ABSTRACT

Cortical surface analysis has gained increased prominence, given its potential implications for neurological and developmental disorders. Traditional vision diffusion models, while effective in generating natural images, present limitations in capturing intricate development patterns in neuroimaging due to limited datasets. This is particularly true for generating cortical surfaces where individual variability in cortical morphology is high, leading to an urgent need for better methods to model brain development and diverse variability inherent across different individuals. In this work, we proposed a novel diffusion model for the generation of cortical surface metrics, using modified surface vision transformers as the principal architecture. We validate our method in the developing Human Connectome Project (dHCP) with results suggesting that our model demonstrates excellent performance in capturing the intricate details of evolving cortical surfaces. Furthermore, our model can generate high-quality realistic samples of cortical surfaces conditioned on postmenstrual age (PMA) at scan.

Index Terms— Diffusion models, cortical surface, generation models

1. INTRODUCTION

The human cerebral cortex is a highly-convoluted sheet of grey matter that is best modeled as a surface [1, 2, 3]. As one of the most highly evolved areas of the brain relative to non-human primates, cortical function underpins many aspects of higher-order cognition and is implicated in many neurological and psychiatric disorders [4, 5]. Unfortunately, localising signs of pathology in individual brains can be extremely challenging due to the scale of variation of human cortical organisation [6, 7, 8], which obscures subtle disease. Therefore, a primary goal of translational neuroimaging is to develop methods that accurately disentangle healthy variation from pathology.

One approach that has gained recent prominence is normative modeling. Here the objective is to learn a generative model that encodes how brains vary normally relative to continuous phenotypes such as age or behavioural scores, from which signs of disease may be detected as outliers from the model [9, 10]. Classically normative models of cortical vari-

ation have been fit with Gaussian Process Regression (GPR) [9, 10] or Generative Additive Models of Location Scale and Shape (GAMLSS) [11]. However, these require hand engineering of imaging features, generally using traditional image processing pipelines that combine diffeomorphic image registration with label propagation of cortical areas from population average templates. Approaches that have been shown repeatedly to under-estimate the full scale of cortical variation [3].

A potentially more powerful approach is to use deep generative models to encode normal brain variation and disentangle it from disease [12]. To this end, denoising Diffusion Probabilistic Models (DDPM) [13] have recently emerged as extremely powerful generators of natural images. Several works [14, 15] have already gained great success in adapting diffusion models to non-Euclidean data, using Stochastic Differential Equations (SDE) to approximate samples on manifolds, but focusing on simple mesh and manifolds generation. However, modeling cortical surfaces requires using high-resolution grids which are not feasible with current methodologies.

To address this problem, we chose to build from recent work on the development of surface vision transformers (SiT) [16]. These have been validated as powerful encoders of cortical feature maps, outperforming surface convolutional approaches to demonstrate state-of-the-art performance of cortical phenotype regression tasks [16]. In this paper we demonstrate that, with the use of an SiT as a backbone for DDPM generation, it is possible to conditionally generate feature maps that accurately simulate cortical neurodevelopment.

2. METHOD

2.1. DDPM formulation

The basis of a DDPM [13] is a sequential diffusion model. This is essentially a forward diffusion process that operates as a Markov chain, incrementally applying Gaussian noise with variance $\beta_t \in (0, 1)$ to the original data distribution $q(x_0)$.

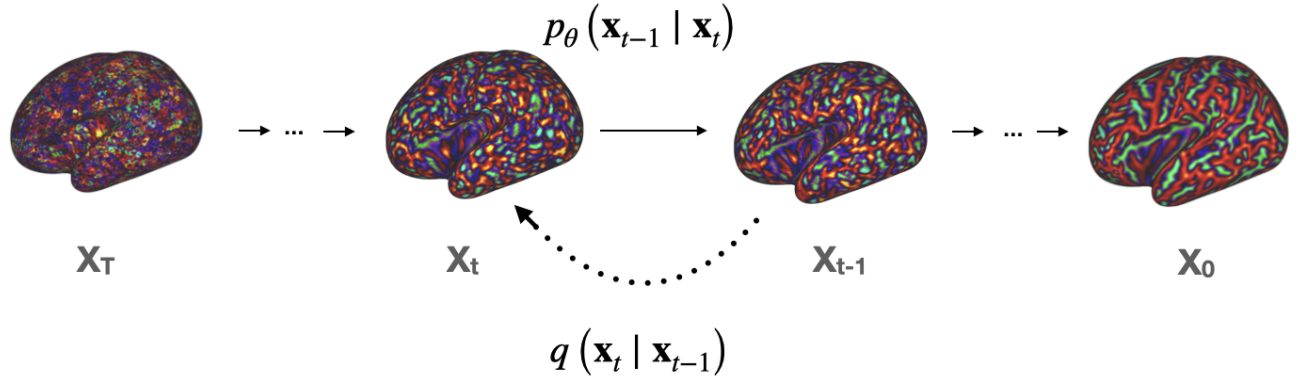


Fig. 1. The directed graphical model of diffusion process on cortical surface

The forward transformation can be represented as follows:

$$q(x_{1:T} | x_0) = \prod_{t=1}^T q(x_t | x_{t-1}) \quad (1)$$

$$q(x_t | x_{t-1}) = \mathcal{N}(x_t; \sqrt{1 - \beta_t}x_{t-1}, \beta_t \mathbf{I}) \quad (2)$$

With x_0 representing the initial data, and $x_{1:T} = \{x_1, x_2, \dots, x_T\}$ representing the latent variables, generated from incremental addition of Gaussian noise (Eq 2). Generation of the diffusion model is learning to reverse the process by using a neural network (ϵ_θ) to iteratively denoise samples over time-steps t . The output of the model is a prediction of the statistics of the distribution: $p_\theta(x_{t-1} | x_t)$:

$$p_\theta(x_{t-1} | x_t) = \mathcal{N}(\mu_\theta(x_t), \Sigma_\theta(x_t)) \quad (3)$$

This model is trained with the variation lower bound of the log-likelihood of x_0 , reducing:

$$\mathcal{L}(\theta) = -p(x_0 | x_1) + \sum_t \mathcal{D}_{KL}(q(x_{t-1} | x_t, x_0) || p_\theta(x_{t-1} | x_t)) \quad (4)$$

As both q and p_θ are Gaussian noise, \mathcal{D}_{KL} can be evaluated from the mean and covariance of two distributions. So the noise prediction network ϵ_θ can be trained easily from the mean-squared error between the predicted noise $\epsilon_\theta(x_t)$ and the sampled Gaussian noise ϵ_t . To generate a sample through the process, an initial point is drawn from $p(x_T)$ with the same dimensions as the original training data x_0 . Then samples $\{x_{T-1}, x_{T-2} \dots x_1\}$ are sequentially denoised by the ϵ_θ until the model approximates the original data point x_0 .

2.2. Surface Diffusion Model

In this paper, samples $x_0 \in \mathbb{R}^{40962 \times 1}$ represent cortical curvature maps, projected to a regular, sixth-order icospheric grid 40962 regularly spaced vertices.

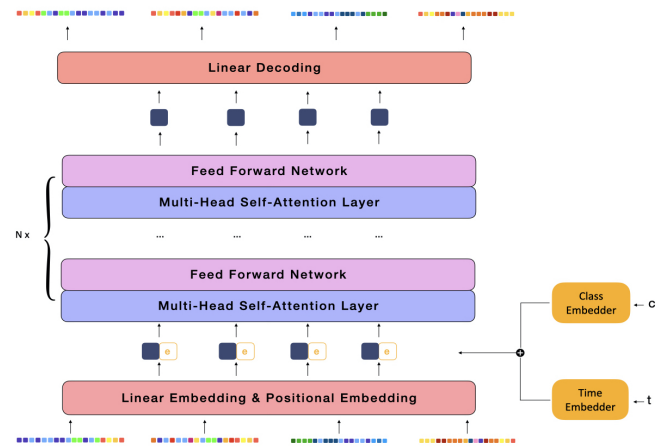


Fig. 2. The figure shows the architecture of the cortical surface diffusion model. First, the flattened input will be projected by linear embedding. Then, positional embedding and condition embeddings (class embedding and time embedding) would be added to the input tokens. After N transformer blocks, the prediction of noise would be projected out by the linear decoding layer.

2.2.1. Surface Vision Transformer

The SiT [16] translates surface understanding to a sequence-to-sequence learning paradigm by tessellating cortical feature maps (sampled on a regular high resolution spherical icosahedral grid) according to regular triangular subdivisions of a lower resolution icosahedron. In this paper, we use ico6 to represent the data, and ico2 ($I_2 = (V_2, F_2)$, $|V_2| = 162$ vertices and $|F_2| = 320$) for sampling. Each patch is generated from the intersection of vertices (V_p) from ico6 that overlap with each face of ico2, which results in a sequence of 320 patches, each of $V_p = 153$ vertices. This generates a sequence of $|F_2|$ flattened patches

of length V_p : $\tilde{X} = [\tilde{X}_1^{(0)}, \dots, \tilde{X}_{|F_2|}^{(0)}] \in R^{|F_2| \times V_p}$, which is first projected onto a D -dimensional sequence of tokens $X^{(0)} = [X_1^{(0)}, \dots, X_{|F_2|}^{(0)}] \in R^{|F_2| \times D}$, using a trainable linear layer (see Figure 2). Positional embedding is then added to encode spatial information about the sequence of tokens. The data is then passed through N vision transformer blocks, each composed of a multi-head self-attention layer and a feed-forward network (for more details of implementation see [16]).

2.2.2. Decoding

In its original form, the SiT was designed for classification or regression [16]. To support iterative prediction of noise and diagonal covariance, at the same resolution as the original data, we extend the network with a layer norm (adaptive if using adaLN) and a standard linear layer to decode each token into $N \times (2V_p)$. Finally, the decoded tokens are rearranged into their original spatial layout to regenerate surface maps.

2.2.3. Conditioning

Following the DDPM formulation in the previous section, samples are iteratively denoised through the SiT, with noise at each iteration parametrized by iteration parameter t . At the same time, we seek to further condition the model on the postmenstrual age of our samples a . This is achieved by appending a and t as additional tokens in the input sequence: adding them into both surface input tokens before the SiT (see Figure 2).

Conditional generation of new samples is supported through use of classifier-free guidance [17]. This approach requires both conditioned $p_\theta(\mathbf{x} | c)$ and unconditioned $p_\theta(\mathbf{x})$ predictions to be generated from the same network (i.e. parametrized as $\epsilon_\theta(\mathbf{x}_t, t, c)$ and $\epsilon_\theta(\mathbf{x}_t, t)$) allowing the gradient of an implicit classifier to be represented as follows:

$$\nabla_{\mathbf{x}_t} \log p(c | \mathbf{x}_t) = \nabla_{\mathbf{x}_t} \log p(\mathbf{x}_t | c) - \nabla_{\mathbf{x}_t} \log p(\mathbf{x}_t) \quad (5)$$

In this setting, classifier-free guidance can be used to encourage the sampling procedure to find x such that $\log p(c | x)$ is high. This method enables the surface diffusion model to generate target samples without module modification and the results have shown its performance on surface data.

3. EXPERIMENTS AND RESULTS

3.1. Data

Data from the developing Human Connectome Project (dHCP) consists of cortical surface meshes and metrics (sulcal depth, curvature, cortical thickness, and T1w/T2w myelination) derived from T1- and T2-weighted magnetic resonance images (MRI) using the dHCP structural pipeline [18]. We use 530 scans from term (born after 37 weeks gestation) and preterm

neonates (born before 37 weeks), covering postmenstrual age (PMA) at scan between 24 to 45 weeks. In this experiment, we only use the curvature map. Training, test, and validation sets were allocated in the ratio of 423:54:53 examples.

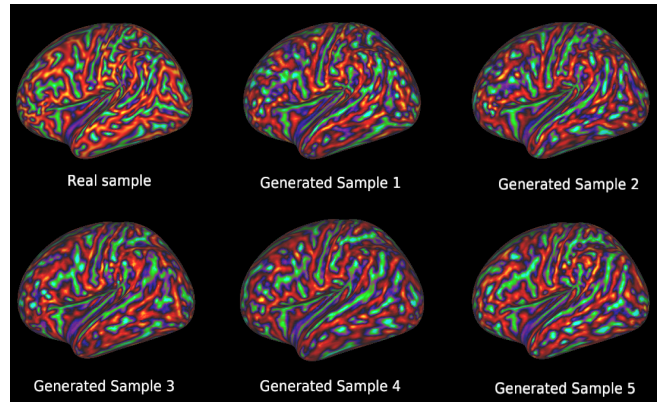


Fig. 3. Unconditional generated curvature surface compared with real sample

3.2. Implementation Details

Training The SiT transformer backbone was implemented with the same size of SiT-small from [16], 12 layers, 6 heads, 384 hidden sizes, and 768 Multi-Layer Perception (MLP) sizes. We train both unconditional and conditional diffusion models with AdamW [19, 20] using standard weight initialization techniques from SiT, except for the final linear (decoding) layer, which is initialised with zeros. Training was implemented with a constant learning rate of 1×10^{-4} , no weight decay, and a batch size of 180 on NVIDIA 3090 with 24 GB memory. Following common practice in the generative modeling literature, we maintain an exponential moving average (EMA) of surface diffusion weights with a training decay of 0.9999.

3.3. Evaluation of Conditional Generation

The model was validated through visual inspection and training of an independent SiT regression model which evaluated whether the generated samples convincingly represent curvature maps of a specific PMA. This regression model was trained on the same data set used for generation, with PMA as the target variable. The proposed surface DDPM was used to generate 20 synthetic examples for each week, from 27 weeks to 44 weeks. The results in table 3.3 report mean absolute error for PMA predictions obtained on ground truth testing data and on synthetic data. Visual examples are shown in Fig 4. Together these results suggest that the proposed model is generating highly realistic cortical curvature maps that can be realistically conditioned on PMA.

	Ground Truth	Synthetic
MAE	0.59 ± 0.51	0.80 ± 0.50
r2	0.96	0.96

Table 1. Prediction results on dHCP test and synthetic data for the PMA regression task. Mean Absolute Error (MAE) with standard deviation are reported, as well as R^2 score.

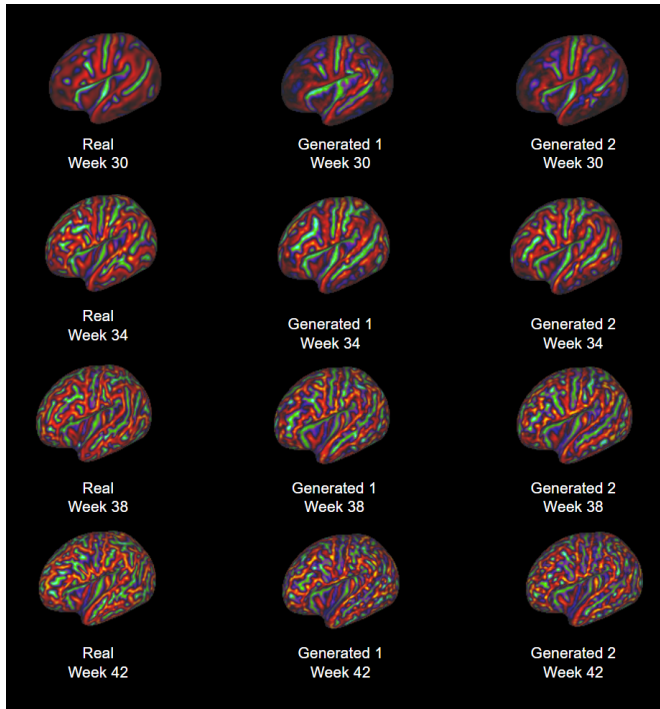


Fig. 4. Samples of cortical surfaces generated by surface diffusion model conditioned on birth age of 30, 34, 38 and 42 weeks, compared to the real samples in dHCP dataset (First line)

4. CONCLUSION

This paper presents a general cortical surface diffusion generative model validated on conditioned generation of cortical curvature maps across neurodevelopment. The generated samples demonstrate that surface diffusion can capture expressive features on the surface sufficiently well to sensitively model the rapid changes in cortical curvature that occur across late gestation. One major contributing factor is the incorporation of a surface vision transformer model, which has previously been shown to outperform surface convolution for cortical phenotype regression. While the results demonstrate considerable potential, the model in its current form is limited to synthesis of entirely novel samples and cannot intervene, or translate the class of individual examples. Future work will look at the towards frameworks for image-to-image translation [12, 21, 22] and deep causal modelling [23]. This would create opportunities for the development of networks

suitable to anomaly detection of focal cortical malformations (such as epileptogenic lesions [24]), modelling of cortical atrophy in dementia [12], or investigation of the subtle impacts of preterm birth on cortical development [21, 22].

5. ACKNOWLEDGMENTS

We would like to acknowledge funding from King’s-China Scholarship(K-CSC) PhD Scholarship program. Data were provided by the developing Human Connectome Project. We are grateful to the families who generously supported this trial.

References

- [1] Bruce Fischl, Martin I Sereno, Roger BH Tootell, and Anders M Dale, “High-resolution intersubject averaging and a coordinate system for the cortical surface,” *Human brain mapping*, vol. 8, no. 4, pp. 272–284, 1999.
- [2] Emma C Robinson, Saad Jbabdi, Matthew F Glasser, Jesper Andersson, Gregory C Burgess, Michael P Harms, Stephen M Smith, David C Van Essen, and Mark Jenkinson, “Msm: a new flexible framework for multimodal surface matching,” *Neuroimage*, vol. 100, pp. 414–426, 2014.
- [3] Matthew F Glasser, Stephen M Smith, Daniel S Marcus, Jesper LR Andersson, Edward J Auerbach, Timothy EJ Behrens, Timothy S Coalson, Michael P Harms, Mark Jenkinson, Steen Moeller, et al., “The human connectome project’s neuroimaging approach,” *Nature neuroscience*, vol. 19, no. 9, pp. 1175–1187, 2016.
- [4] Tomáš Paus, Matcheri Keshavan, and Jay N Giedd, “Why do many psychiatric disorders emerge during adolescence?,” *Nature reviews neuroscience*, vol. 9, no. 12, pp. 947–957, 2008.
- [5] James M Roe, Didac Vidal-Piñeiro, Øystein Sørensen, Andreas M Brandmaier, Sandra Düzel, Hector A Gonzalez, Rogier A Kievit, Ethan Knights, Simone Kühn, Ulman Lindenberger, et al., “Asymmetric thinning of the cerebral cortex across the adult lifespan is accelerated in alzheimer’s disease,” *Nature communications*, vol. 12, no. 1, pp. 721, 2021.
- [6] Matthew F Glasser, Timothy S Coalson, Emma C Robinson, Carl D Hacker, John Harwell, Essa Yacoub, Kamil Ugurbil, Jesper Andersson, Christian F Beckmann, Mark Jenkinson, et al., “A multi-modal parcellation of human cerebral cortex,” *Nature*, vol. 536, no. 7615, pp. 171–178, 2016.

- [7] Ru Kong, Jingwei Li, Csaba Orban, Mert R Sabuncu, Hesheng Liu, Alexander Schaefer, Nanbo Sun, Xi-Nian Zuo, Avram J Holmes, Simon B Eickhoff, et al., “Spatial topography of individual-specific cortical networks predicts human cognition, personality, and emotion,” *Cerebral cortex*, vol. 29, no. 6, pp. 2533–2551, 2019.
- [8] Evan M Gordon, Timothy O Laumann, Adrian W Gilmore, Dillan J Newbold, Deanna J Greene, Jeffrey J Berg, Mario Ortega, Catherine Hoyt-Drazen, Caterina Gratton, Haoxin Sun, et al., “Precision functional mapping of individual human brains,” *Neuron*, vol. 95, no. 4, pp. 791–807, 2017.
- [9] Andre F Marquand, Ieud Rezek, Jan Buitelaar, and Christian F Beckmann, “Understanding heterogeneity in clinical cohorts using normative models: beyond case-control studies,” *Biological psychiatry*, vol. 80, no. 7, pp. 552–561, 2016.
- [10] Saige Rutherford, Seyed Mostafa Kia, Thomas Wolfers, Charlotte Frazz, Mariam Zabihi, Richard Dinga, Pierre Berthet, Amanda Worker, Serena Verdi, Henricus G Ruhe, et al., “The normative modeling framework for computational psychiatry,” *Nature protocols*, vol. 17, no. 7, pp. 1711–1734, 2022.
- [11] Richard AI Bethlehem, Jakob Seidlitz, Simon R White, Jacob W Vogel, Kevin M Anderson, Chris Adamson, Sophie Adler, George S Alexopoulos, Evdokia Anagnostou, Ariosky Areces-Gonzalez, et al., “Brain charts for the human lifespan,” *Nature*, vol. 604, no. 7906, pp. 525–533, 2022.
- [12] Cher Bass, Mariana Da Silva, Carole Sudre, Logan ZJ Williams, Helena S Sousa, Petru-Daniel Tudosiu, Fidel Alfaro-Almagro, Sean P Fitzgibbon, Matthew F Glasser, Stephen M Smith, et al., “Icam-reg: Interpretable classification and regression with feature attribution for mapping neurological phenotypes in individual scans,” *IEEE Transactions on Medical Imaging*, vol. 42, no. 4, pp. 959–970, 2022.
- [13] Jonathan Ho, Ajay Jain, and Pieter Abbeel, “Denoising diffusion probabilistic models,” *Advances in neural information processing systems*, vol. 33, pp. 6840–6851, 2020.
- [14] Zhen Liu, Yao Feng, Michael J Black, Derek Nowrouzezahrai, Liam Paull, and Weiyang Liu, “Meshdiffusion: Score-based generative 3d mesh modeling,” *arXiv preprint arXiv:2303.08133*, 2023.
- [15] Chin-Wei Huang, Milad Aghajohari, Joey Bose, Prakash Panangaden, and Aaron C Courville, “Riemannian diffusion models,” *Advances in Neural Information Processing Systems*, vol. 35, pp. 2750–2761, 2022.
- [16] Simon Dahan, Abdulah Fawaz, Logan Z. J. Williams, Chunhui Yang, Timothy S. Coalson, Matthew F. Glasser, A. David Edwards, Daniel Rueckert, and Emma C. Robinson, “Surface vision transformers: Attention-based modelling applied to cortical analysis,” 2022.
- [17] Jonathan Ho and Tim Salimans, “Classifier-free diffusion guidance,” *arXiv preprint arXiv:2207.12598*, 2022.
- [18] Antonios Makropoulos, Emma C. Robinson, Andreas Schuh, Robert Wright, Sean Fitzgibbon, Jelena Bozek, Serena J. Counsell, Johannes Steinweg, Katerina Vecchiato, Jonathan Passerat-Palmbach, Gabriel Lenz, Filippo Mortari, Tihomir Tenev, Eugene P. Duff, Matteo Bastiani, Lucilio Cordero-Grande, Emer Hughes, Nora Tusor, J. Donald Tournier, Jana Hutter, Anthony N. Price, Rui Pedro A. G. Teixeira, Maria Murgasova, Sarah Victor, Christopher Kelly, Mary A. Rutherford, Stephen M. Smith, A. David Edwards, Joseph V. Hajnal, Mark Jenkinson, and Daniel Rueckert, “The developing human connectome project: A minimal processing pipeline for neonatal cortical surface reconstruction,” *Neuroimage*, vol. 173, pp. 88–112, 2018.
- [19] Ilya Loshchilov and Frank Hutter, “Decoupled weight decay regularization,” *arXiv preprint arXiv:1711.05101*, 2017.
- [20] Diederik P Kingma and Jimmy Ba, “Adam: A method for stochastic optimization,” *arXiv preprint arXiv:1412.6980*, 2014.
- [21] Abdulah Fawaz, Logan ZJ Williams, A David Edwards, and Emma C Robinson, “A deep generative model of neonatal cortical surface development,” in *Annual Conference on Medical Image Understanding and Analysis*. Springer, 2022, pp. 469–481.
- [22] Abdulah Fawaz, Saga NB Masui, Logan Zane John Williams, Simon Dahan, David Edwards, and Emma Claire Robinson, “Surface generative modelling of neurodevelopmental trajectories,” *bioRxiv*, pp. 2023–10, 2023.
- [23] Pedro Sanchez and Sotirios A Tsaftaris, “Diffusion causal models for counterfactual estimation,” *arXiv preprint arXiv:2202.10166*, 2022.
- [24] Hannah Spitzer, Mathilde Ripart, Abdulah Fawaz, Logan ZJ Williams, MELD project, Emma C Robinson, Juan Eugenio Iglesias, Sophie Adler, and Konrad Wagstyl, “Robust and generalisable segmentation of subtle epilepsy-causing lesions: A graph convolutional approach,” in *International Conference on Medical Image Computing and Computer-Assisted Intervention*. Springer, 2023, pp. 420–428.